# Heavy quarkonia, heavy-light tetraquarks, and the chiral quark-soliton model

Maciej Kucab[*] and Michał Praszałowicz[†]
*Institute of Theoretical Physics, Jagiellonian University, S. Łojasiewicza 11, 30-348 Kraków, Poland*

(Received 11 February 2024; accepted 13 March 2024; published 8 April 2024)

We apply the chiral quark-soliton model, used previously to describe baryons with one heavy quark, to the case of heavy tetraquarks. We argue that the model is insensitive to the nature of the heavy object bound by the soliton, i.e., to its mass and spin. Therefore, a heavy quark can be replaced by an antidiquark without modifying the soliton background. Diquark dynamics is taken into account by means of the nonrelativistic Schrödinger equation with the Cornell potential. We fix the Cornell potential parameters from the charmonia and bottomonia spectra. We first compute $B_c$-meson masses to check our fitting procedure, and then compute diquark masses by appropriately rescaling color factors in the Cornell potential. We then compute tetraquark masses and confirm previous findings that only $bb$ tetraquarks are bound.

DOI: 10.1103/PhysRevD.109.076005

## I. INTRODUCTION

In 2022, the LHCb Collaboration discovered the doubly charmed tetraquark $\mathcal{T}_{cc}$ [1,2] in the $D^0D^0\pi^+$ invariant mass distribution. The $\mathcal{T}_{cc}$ mass of 3875 MeV is just below the $D^0D^*$ threshold. The LHCb discovery triggered theoretical activity. We refer the reader to a review on multiquark states, both experimental and theoretical, before the $\mathcal{T}_{cc}^+$ discovery [3] and after the LHCb paper [4] (and references therein).

Motivated by the $\mathcal{T}_{cc}^+$ discovery, one of us proposed a model [5] where heavy tetraquarks $\mathcal{T}_{QQ}$ were described as a chiral soliton and a $\bar{Q}\,\bar{Q}$ diquark. The chiral quark-soliton model ($\chi$QSM) has been formulated to describe light baryons (see Ref. [6] and Refs. [7–9] for review) where the soliton is constructed from $N_c$ light quarks. It has been argued in Refs. [10–14] that in the large-$N_c$ limit mean chiral fields of the soliton do not change if one valence quark is replaced by a heavy quark $Q$. Such a replacement leads to a successful phenomenological description of baryons with one heavy quark [10,12,13]. Since after removing one light quark the soliton is in a color $\bar{\mathbf{3}}$ (or, more precisely, a color representation $\mathcal{R}$ corresponding to an antisymmetric product on $N_c - 1$ quarks), adding a heavy quark in color $\mathbf{3}$ leads to multiplets of heavy baryons that are conveniently characterized by $\mathrm{SU}(3)_{\mathrm{flavor}}$ quantum numbers of $N_c - 1$ light quarks (i.e., a diquark for $N_c = 3$). In this respect, the $\chi$QSM is identical to a quark model.

It has been shown in Refs. [10–14] that for a successful phenomenological description of heavy baryons, it is enough to add the masses of a soliton and a heavy quark, and include a spin-spin interaction between the two. The model describes well both charm and bottom baryon spectra [10,12,13], indicating that binding effects of the soliton-$Q$ system do not depend on the heavy-quark mass. We present quantitative evidence for this independence in Sec. II. This observation suggests that an equally good description should hold for a system where a heavy quark is replaced by a heavy (anti)diquark $\bar{Q}_1\bar{Q}_2$ in the color triplet. In Ref. [5] and earlier in Ref. [15] we considered the case where $Q_1 = Q_2$.

In the present paper, we study a more general case where heavy quarks[1] can be either identical or different, i.e., we consider $cc$, $bb$, and $cb$ diquarks. The diquark dynamics is modeled by a nonrelativistic Schrödinger equation with the Cornell potential [16,17] and the spin-spin interaction of heavy quarks, which was not explicitly included in Ref. [5]. Since we are only interested in the diquark ground states, angular momentum and tensor terms are neglected. We use as an input $J/\psi$, $\eta_c$, $\Upsilon$, and $\eta_b$ mesons to constrain the Cornell potential parameters and quark masses. As a result, the masses of $b\bar{c}$ or $\bar{c}b$ mesons are predictions and actually test our approach. The model reproduces very well the two known $B_c^+(1S_0, 6274.5)$ and $B_c^\pm(2S_0, 6871.2)$ mesons [18].

[*]maciej.kucab@student.uj.edu.pl
[†]michal.praszalowicz@uj.edu.pl



[1]In what follows, we use the term *quark* or *diquark* to refer to either $Q_1$, $Q_2$ or $\bar{Q}_1, \bar{Q}_2$.

Once the Cornell potential parameters are fixed, we can compute the diquark masses by coupling quark color charges to an antitriplet rather than to a singlet, as in the meson case. Finally, by adding the diquark mass to the soliton mass with the diquark-soliton spin interaction, we obtain predictions for the tetraquark masses.

Two heavy quarks of the same flavor (say, $cc$ or $bb$) can form a color antitriplet (antisymmetric in color) provided they are symmetric in spin [19]. Therefore, they form a tight object of spin 1. Hence, two heavy antiquarks are in color 3 and spin 1, behaving as a spin-1 heavy *quark*. Additionally, a $cb$ diquark can be in a state of spin 0, which is antisymmetric in flavor.

Heavy tetraquarks were theoretically anticipated many years ago [20,21] on the basis of heavy-quark symmetry [22] (see also [23–29]). Probably the first estimate of the tetraquark mass was done by Lipkin in 1986 [30] (although the fourfold heavy tetraquarks were discussed even earlier in 1982 [31]). A phenomenological analysis of heavy tetraquarks was recently carried out in Ref. [32]. In fact, our model is very reminiscent of the one in Ref. [32] where tetraquark mass formulas are identical to those for heavy baryons, with some modification due to the integer or zero spin of the heavy diquark.

Our findings can be summarized as follows. The diquark dynamics restricted to the $s$ channel, modeled by the Cornell potential, describes well charmonia and bottomonia ground states and first excited states; however, the value of the string tension giving the best fit is different in the $c$ and $b$ channels. This is consistent with global fits [17]. Using the parameters fixed from meson spectra, we compute diquark masses and the tetraquark masses. We find that only $bb$ tetraquarks are bound.

In Sec. II we introduce the $\chi$QSM and discuss its application to heavy baryons. We present arguments that the soliton properties do not depend on the heavy-quark mass. Next, we introduce a classification of the tetraquark states according to the SU(3) content of the light subsystem and derive pertinent mass formulas. In Sec. III we solve the Schrödinger equation for heavy mesons and fix the Cornell potential parameters. As a test, we compute $B_c$ mesons masses and then the diquark masses. Numerical results for the tetraquark masses are presented in Sec. IV. We summarize our findings in Sec. V.

## II. CHIRAL QUARK-SOLITON MODEL

In this section, we briefly recall the main features of the $\chi$QSM (see Refs. [6–9] and references therein). We discuss the application of the $\chi$QSM first to heavy baryons and then to tetraquarks.

### A. Heavy baryons

The soliton in the current approach corresponds to a stable aggregate configuration of valence quarks and a fully occupied Dirac sea. In the large-$N_c$ limit, $N_c$ (or $N_c - 1$) relativistic valence quarks polarize the Dirac sea, which in turn modifies the valence-quark levels, which in turn distort the sea, until a stable soliton configuration is reached [33,34]. Quantum numbers are generated by the quantization of zero modes, corresponding to the rotations in the SU(3) space and in the configuration space. In the chiral limit, the soliton energy is given by a formula analogous to the quantum-mechanical symmetric top [35–37],

$$E_{\mathrm{sol}} = M_{\mathrm{sol}} + \frac{J(J+1)}{2I_1} + \frac{C_2(p,q) - J(J+1) - 3/4Y'^2}{2I_2}. \tag{1}$$

Here $M_{\mathrm{sol}}$ is a classical soliton mass, $I_{1,2}$ stand for the moments of inertia, $C_2(p,q)$ is the SU(3) Casimir for the baryon multiplet, and $J$ corresponds to the soliton spin. In the case of $N_c - 1$ valence quarks, $Y' = (N_c - 1)/3 = 2/3$ in the real world, and the allowed SU(3) representations are $\bar{\mathbf{3}}$ with spin $J = 0$ and $\mathbf{6}$ with spin $J = 1$ [10].

The Hamiltonian (1) has to be supplemented by the chiral-symmetry-breaking part (which can be found in Ref. [38]) and the hyperfine splitting part [10],

$$H_{SQ} = \frac{2}{3}\frac{\varkappa}{m_Q}\boldsymbol{J}\cdot\boldsymbol{S}_Q, \tag{2}$$

where $\boldsymbol{J}$ and $\boldsymbol{S}_Q$ stand for the soliton and the heavy quark or diquark spin, respectively. Since the spin of the $\bar{\mathbf{3}}$ representation is zero, there is no hyperfine splitting in this case. The chiral-symmetry-breaking part leads to mass splittings proportional to the baryon hypercharge, denoted below by $\delta_{\bar{\mathbf{3}},\mathbf{6}}$ [10].

Therefore, the mass formulas for heavy baryons read as follows [10,15]:

$$\begin{aligned} M_{B_Q,\bar{\mathbf{3}}} &= m_Q + M_{\mathrm{sol}} + \frac{1}{2I_2} + \delta_{\bar{\mathbf{3}}} Y_B, \\ M_{B_Q,\mathbf{6},s} &= m_Q + M_{\mathrm{sol}} + \frac{1}{2I_2} + \frac{1}{I_1} + \delta_{\mathbf{6}} Y_B \\ &\quad + \frac{\kappa}{m_Q}\begin{cases} -2/3 & \text{for } s = 1/2, \\ +1/3 & \text{for } s = 3/2. \end{cases} \end{aligned} \tag{3}$$

Here $Y_B$ stands for the hypercharge of a given baryon. In the case of antitriplet, soliton spin $J = 0$ and the corresponding heavy baryons have spin $1/2$, for sextet $J = 1$ and the corresponding baryons have spin $1/2$ and $3/2$.

It was shown in Refs. [10,12,13] that the above mass formulas lead to a very good description of heavy baryon spectra. Below we examine the main features of our approach:

(1) Soliton properties are independent of the heavy-quark mass.

(2) Soliton properties do not depend on the spin coupling between a soliton and a heavy quark.
(3) Hyperfine splittings are proportional to $1/m_Q$.

Averaging over spin and hypercharge, we define the mean antitriplet and sextet masses:

$$M^Q_{\bar{\mathbf{3}}} = m_Q + M_{\rm sol} + \frac{1}{2I_2} = 2408.2|_c = 5736.2|_b,$$
$$M^Q_{\mathbf{6}} = m_Q + M_{\rm sol} + \frac{1}{2I_2} + \frac{1}{I_1} = 2579.4|_c = 5906.5|_b, \quad (4)$$

in MeV.

As discussed in Ref. [5], one can form differences of average multiplet masses between the $b$ and $c$ sectors to compute heavy-quark the mass difference (in MeV),

$$m_b - m_c = 3328|_{\bar{\mathbf{3}}} = 3327|_{\mathbf{6}}, \quad (5)$$

which illustrates properties 1 and 2 above.

Furthermore, one can estimate the hyperfine splitting parameter entering (2):

$$\frac{\varkappa}{m_c} = 64.6|_{\Sigma_c} = 67.2|_{\Xi_c} = 70.7|_{\Omega_c},$$
$$\frac{\varkappa}{m_b} = 19.4|_{\Sigma_b} = 18.8|_{\Xi_b} \quad (6)$$

(in MeV). From these estimates, we get

$$\frac{m_c}{m_b} \simeq 0.27\text{–}0.30 \quad (7)$$

with the average value of 0.283, which is close to the PDG value of 0.3 [18] in agreement with properties 2 and 3.

From Eqs. (5) and (7), one can estimate the heavy-quark masses as

$$m_c = 1206\text{–}1426~\text{MeV},$$
$$m_b = 4533\text{–}4753~\text{MeV}, \quad (8)$$

which are a bit higher (especially $m_b$) than the values reported by the Particle Data Group (PDG) [18]. For $m_c/m_b = 0.283$, we get $m_c = 1314.1$ MeV and $m_b = 4641.5$ MeV, which is still lower than the effective values used in Ref. [39]. However, one should remember that the quark masses in effective models may differ from the QCD estimates in the $\overline{\rm MS}$ scheme.

In Ref. [10], the heavy-quark dependence of the mass formulas (3) was tested by computing the nonstrange moment of inertia from the $\mathbf{6} - \bar{\mathbf{3}}$ average mass differences where both spin and hypercharge splittings cancel:

$$\frac{1}{I_1} = M^Q_{\mathbf{6}} - M^Q_{\bar{\mathbf{3}}} = 171.2|_c = 170.3|_b \quad (9)$$

(in MeV). As we see from (9), the heavy-quark masses cancel almost exactly, which again illustrates properties 1 and 2. We can therefore safely assume that the formulas (5) are valid for any heavy object in a color triplet replacing $Q$.

### B. Heavy tetraquarks

Since heavy tetraquarks in the $\chi$QSM are formed by replacing a heavy quark with a diquark, and since the mass of the soliton is independent of the heavy-quark or diquark mass and spin, very simple tetraquark mass formulas emerge, which relate tetraquark masses to the baryon masses [5,16]. The mass formula for the ground-state antitriplet is particularly simple, since the soliton in this case is spinless and the hyperfine splitting (2) is not present,

$$M^{\mathrm{tetra}\bar{\mathbf{3}}}_{\bar{Q}\bar{Q}} = M_{B_Q,\bar{\mathbf{3}}} - m_Q + m_{\bar{Q}\bar{Q}}. \quad (10)$$

Here $M_{B_Q,\bar{\mathbf{3}}}$ stands for $\Lambda_Q(2286.5|_c, 5619.6|_b)$ or the isospin-averaged $\Xi_Q(2469|_c, 5794.5|_b)$ mass, $m_{\bar{Q}\bar{Q}}$ denotes the antidiquark mass (to be discussed in Sec. III D), and $m_Q$ stands for the heavy-quark mass.

In the case of a sextet, since the soliton spin is $J=1$, we have to distinguish two cases when the diquark spin is 0 or 1. It is convenient to introduce spin and isospin-averaged baryon masses:

$$M_{B_Q,\mathbf{6}} = \frac{1}{2T+1}\sum_{T_3}\frac{1}{3}\left(M_{B_Q,\mathbf{6},T_3,1/2} + 2M_{B_Q,\mathbf{6},T_3,3/2}\right) \quad (11)$$

where $B_Q$ stands for $\Sigma_Q(2496.6|_c, 5826|_b)$, $\Xi'_Q(2623.2|_c, 5947.6|_b)$, or $\Omega_Q(2742.3|_c, 6065|_b)^2$ in MeV. The mass formulas read as follows:

$$M^{\mathrm{tetra}\mathbf{6}}_{\bar{Q}\bar{Q}} = M_{B_Q,\mathbf{6}} - m_Q + m_{\bar{Q}\bar{Q}} + C_{\rm spin}\frac{2}{3}\frac{\varkappa}{m_Q}\frac{m_Q}{m_{\bar{Q}\bar{Q}}}, \quad (12)$$

where

$$C_{\rm spin} = \begin{cases} \left.\begin{array}{ll} -2 & \text{for } s=0 \\ -1 & \text{for } s=1 \\ 1 & \text{for } s=2 \end{array}\right\} & \text{for } S_{\bar{Q}\bar{Q}} = 1, \\ \quad 0 \quad \text{for } s=0 & \text{for } S_{\bar{Q}\bar{Q}} = 0. \end{cases} \quad (13)$$

The mass formulas (10) and (12) relate tetraquark masses directly to heavy baryon masses and therefore are fairly model independent. They are analogous to Eq. (1) of Ref. [32]. The spin part was discussed in [40]; however, the hyperfine coupling has not been specified. Here we know the value of $\varkappa/m_{c,b}$ [Eq. (6)], so in order to estimate tetraquark masses we only need the heavy diquark mass $m_{\bar{Q}\bar{Q}}$ for $m_Q$ in the range (8).

---
[2] For $\Omega_b^*$, we take the mass estimate from Ref. [10].

TABLE I. Thresholds for tetraquark decays in MeV. The first column shows the baryon entering the mass formulas (10) and (12), which specifies the tetraquark SU(3) representation. The other columns indicate pertinent diquarks and their spin. If more than one decay channel is possible, only the one with the lowest mass is shown.

| | | $\{\bar{c}\bar{c}\}_1$ | | $\{\bar{b}\bar{b}\}_1$ | | $\{\bar{c}\bar{b}\}_1$ | | | $[\bar{c}\bar{b}]_0$ | |
|---|---|---|---|---|---|---|---|---|---|---|
| | $J^P$ | Channel | Threshold | Channel | Threshold | Channel | Threshold | $J^P$ | Channel | Threshold |
| $\Lambda_Q$ | $1^+$ | $\bar{D}^0 D^{*-}$ | 3875 | $B^+ B^{*0}$ | 10 604 | $\bar{D}^0 B^{*0}$ | 7190 | $0^+$ | $\bar{D}^0 B^0$ | 7144 |
| $\Xi_Q$ | $1^+$ | $\bar{D}^{*0} D_s^-$ | 3976 | $B^{*+} \bar{B}_s^0$ | 10 692 | $\bar{D}^{*0} \bar{B}_s^0$ | 7281 | $0^+$ | $\bar{D}^0 \bar{B}_s^0$ | 7232 |
| | $0^+$ | $D^0 D^0$ | 3730 | $B^+ B^+$ | 10 559 | $\bar{D}^0 B^+$ | 7144 | ... | ... | ... |
| $\Sigma_Q$ | $1^+$ | $D^0 D^{*0}$ | 3872 | $B^+ B^{*+}$ | 10 604 | $\bar{D}^{*0} B^+$ | 7286 | $1^+$ | $\bar{D}^{*0} B^+$ | 7286 |
| | $2^+$ | $D^{*0} D^{*0}$ | 4014 | $B^{*+} B^{*+}$ | 10 649 | $\bar{D}^{*0} B^{*+}$ | 7332 | ... | ... | ... |
| | $0^+$ | $\bar{D}^0 D_s^-$ | 3834 | $B^+ \bar{B}_s^0$ | 10 646 | $\bar{D}^0 \bar{B}_s^0$ | 7232 | ... | ... | ... |
| $\Xi'_Q$ | $1^+$ | $\bar{D}^{*0} D_s^-$ | 3976 | $B^+ \bar{B}_s^{*0}$ | 10 692 | $\bar{D}^0 \bar{B}_s^{*0}$ | 7281 | $1^+$ | $\bar{D}^0 \bar{B}_s^{*0}$ | 7281 |
| | $2^+$ | $\bar{D}^{*0} D_s^{*-}$ | 4120 | $B^{*+} \bar{B}_s^{*0}$ | 10 741 | $\bar{D}^{*0} \bar{B}_s^{*0}$ | 7423 | ... | ... | ... |
| | $0^+$ | $D_s^- D_s^-$ | 3938 | $\bar{B}_s^0 \bar{B}_s^0$ | 10 734 | $D_s^- \bar{B}_s^0$ | 7336 | ... | ... | ... |
| $\Omega_Q$ | $1^+$ | $D_s^- D_s^{*-}$ | 4082 | $\bar{B}_s^0 \bar{B}_s^{*0}$ | 10 783 | $D_s^{*-} \bar{B}_s^0$ | 7480 | $1^+$ | $D_s^{*-} \bar{B}_s^0$ | 7480 |
| | $2^+$ | $D_s^{*-} D_s^{*-}$ | 4226 | $\bar{B}_s^{*0} \bar{B}_s^{*0}$ | 10 832 | $D_s^{*-} \bar{B}_s^{*0}$ | 7529 | ... | ... | ... |

Before proceeding to numerical calculations, we need to know the strong decay thresholds that depend on the $J^P$ quantum numbers, which are listed in Table I.

## III. HEAVY MESONS AND DIQUARKS

### A. Mass formulas

In order to predict the heavy-tetraquark masses, one needs a reliable estimate of the heavy-diquark mass. Following Ref. [5], we use a nonrelativistic Schrödinger equation with the Cornell potential [16,17]

$$V(r) = -\frac{\kappa}{r} + \sigma r + \frac{2}{3} C_{\text{color}} \frac{\alpha_s}{m_1 m_2 r^2} (s_1 \cdot s_2) \delta(r), \tag{14}$$

including the spin-spin interaction, which we treat as a perturbation. Since we are only interested in $s$-wave states, we do not include tensor and spin-orbit interactions. Here $m_{1,2}$ stand for the heavy-quark masses and we also introduce a reduced mass

$$\mu = \frac{m_1 m_2}{m_1 + m_2}, \tag{15}$$

which is equal to $m/2$ for quarks of identical mass $m$. The string tension $\sigma$ should in principle be a universal constant; however, it is known from global analyses that good quality fits require $\sigma$, which is different in the $c$ and $b$ sector [17]. Since the Coulomb part follows from the one-gluon exchange, $\kappa = C_{\text{color}} \alpha_s$, where $C_{\text{color}}$ is a color factor.

Here we adopt units where $\dim[m] = \text{GeV}$, $\dim[r] = 1/\text{GeV}$, $\dim[\sigma] = \text{GeV}^2$, and $\kappa$ is dimensionless.

There is one important practical reason to use the Cornell potential in the present context. For a $Q_1 \bar{Q}_2$ system in a color singlet, $C_{\text{color}} = C_F = 4/3$. In order to compute the diquark masses $Q_1 Q_2$ (or $\bar{Q}_1 \bar{Q}_2$), one has to couple quark color charges to $\bar{\mathbf{3}}$ (or $\mathbf{3}$), and then the color factor is $C_{\text{color}} = C_F/2 = 2/3$ (see, e.g., Table III in Ref. [39]). As this is quite obvious for the Coulomb and spin terms, lattice calculations suggest the same behavior for the confining part [41].

Therefore, once the potential parameters are fixed from the $c\bar{c}$ and $b\bar{b}$ meson spectra, we can compute the diquark masses by rescaling the color factors and the string tension in (14) by a factor of 2.

We are looking for a solution of the Schrödinger equation in terms of a function $u_n(r)$ defined as follows:

$$\psi_{nl=0m=0}(r, \theta, \varphi) = R_0^n(r) Y_{00}(\theta, \varphi) = \frac{u_n(r)}{r} \frac{1}{\sqrt{4\pi}}. \tag{16}$$

It is convenient to introduce a dimensionless variable $\rho$,

$$r = \left(\frac{1}{2\sigma\mu}\right)^{1/3} \rho, \tag{17}$$

and rescaled dimensionless parameters $\lambda$ and $\zeta$,

$$\lambda = \left(\frac{2\mu}{\sigma^{1/2}}\right)^{2/3} \kappa, \qquad \zeta = \left(\frac{2\mu}{\sigma^2}\right)^{1/3} E. \tag{18}$$

With these substitutions, the Schrödinger equation takes the very simple form

$$u'' + \left[\frac{\lambda}{\rho} - \rho + \zeta\right] u = 0. \tag{19}$$

The results for the rescaled energies $\zeta_i$ are shown in the upper panel of Fig. 1. We choose the normalization

$$\int_0^\infty d\rho |u(\rho)|^2 = 1. \tag{20}$$

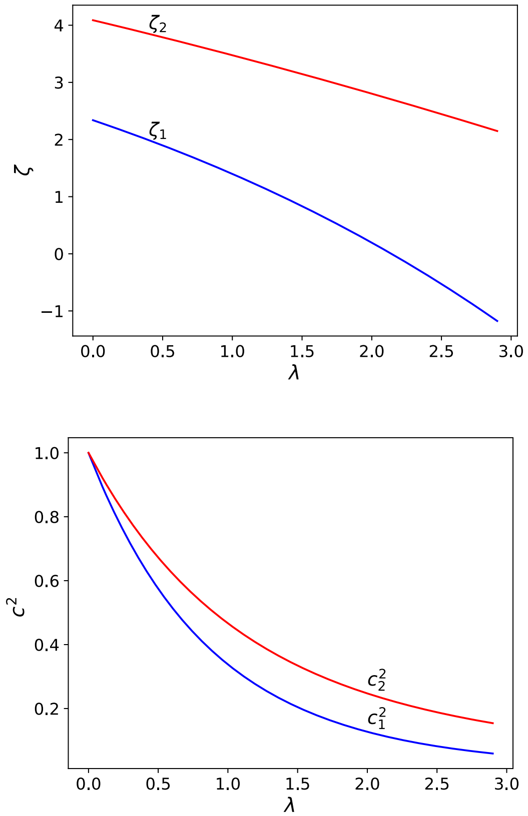


FIG. 1. Dimensionless energies $\zeta_n$ and normalization factors $c_n^2$ for the ground and first excited states as functions of $\lambda$.

Now we need to compute the hyperfine splitting. In the first order of perturbation theory, for $l = 0$ states we have

$$\Delta_{\rm hf}^{(s)} E_n = \frac{2}{3} C_F \alpha_s \frac{2\sigma}{m_1 + m_2} \left( \frac{u_n(\rho)}{\rho}\bigg|_{\rho=0} \right)^2 (s_1 \cdot s_2). \tag{21}$$

In Ref. [5] we solved Eq. (19) semianalytically by treating the Coulomb part as a perturbation, since for $\lambda = 0$ Eq. (19) reduces to the Airy equation. While this method is quite accurate as far as the eigenvalues $\zeta_n$ are concerned, it fails for the hyperfine splitting (21) where the value of the wave function in the origin is needed. Therefore, here we have decided to solve Eq. (19) numerically. Because for $l = 0$ the function $R(r)$ is constant at $r = 0$, the function $u_n(\rho) = c_n \rho + \mathcal{O}(\rho^2)$ for small $\rho$. In Fig. 1 we plot the normalization constants $c_n^2$ for $n = 1$ and 2. As a result, the mass of the $Q_1 \bar{Q}_2$ meson (and its antiparticle) of spin $s$ reads as follows:

$$(M_{Q_1\bar{Q}_2})_n^s = m_1 + m_2 + \left(\frac{\sigma^2}{2\mu}\right)^{1/3} \zeta_n + \frac{2}{3} C_F \alpha_s \frac{2\sigma}{m_1 + m_2} c_n^2 \begin{cases} -3/4 & \text{for } s = 0, \\ +1/4 & \text{for } s = 1. \end{cases} \tag{22}$$

As explained earlier, diquark masses can be computed from the same formula by rescaling $C_F \to C_F/2$ and $\sigma \to \sigma/2$. This rescaling changes the value of the parameter

$$\lambda \to \lambda' = \lambda / 4^{1/3}. \tag{23}$$

Note that the actual value of $\lambda$ in Eq. (19) depends on the system considered, as it depends on $\mu$, both explicitly [Eq. (18)] and implicitly, since $\kappa$ is also a function of $\mu$. For this new value $\lambda'$, we have different energies $\zeta_n'$ and new wave functions leading to a new value of $c_n \to c_n'$. The final mass formula for a diquark is therefore given as follows:

$$(M_{\bar{Q}_1\bar{Q}_2})_n^s = m_1 + m_2 + \left(\frac{\sigma^2}{8\mu}\right)^{1/3} \zeta_n' + \frac{1}{3} C_F \alpha_s \frac{\sigma}{m_1 + m_2} c_n'^2 \begin{cases} -3/4 & \text{for } s = 0, \\ +1/4 & \text{for } s = 1. \end{cases} \tag{24}$$

Note that for identical quarks the $s = 0$ configuration is Pauli forbidden. In practice, we consider only the two lowest states: the ground state $n = 1$ and the first radially excited state $n = 2$.

### B. Fitting procedure

As the first step, we use Eq. (22) to fix potential parameters from the $n = 1$ states shown in Table II. We have decided to perform our own dedicated fits rather than use the global fits to all known quarkonia states. This is because we are only interested in the ground states for both mesons and diquarks; however, we will see that $n = 2$ excited states are quite well reproduced within the accuracy of the present approach.

From Table II we find the average $n = 1$ masses,

$$\bar{M}_{c\bar{c}} = \frac{3M_{J/\psi} + M_{\eta_c}}{4} = 3.069 \text{ GeV},$$
$$\bar{M}_{b\bar{b}} = \frac{3M_{\Upsilon} + M_{\eta_b}}{4} = 9.445 \text{ GeV}, \tag{25}$$

and average $n = 1$ spin splittings,

$$\delta_{\rm hf} E(c\bar{c}) = 113 \text{ MeV}, \qquad \delta_{\rm hf} E(b\bar{b}) = 61 \text{ MeV}. \tag{26}$$

We first numerically solve Eq. (19) for $0 \le \lambda \le 3$ and tabulate the energy levels $\zeta_{1,2}(\lambda)$ and constants $c_{1,2}(\lambda)$.

TABLE II. Lowest quarkonia states used in the fits of the Cornell potential parameters.

| $(n, s)$ | | MeV | | MeV |
|---|---|---|---|---|
| (1, 0) | $\eta_c(1S_0)$ | 2984 | $\eta_b(1S_0)$ | 9399 |
| (1, 1) | $J/\psi(1S_1)$ | 3097 | $\Upsilon(1S_1)$ | 9460 |
| (2, 0) | $\eta_c(2S_0)$ | 3637 | $\eta_b(2S_0)$ | 9999 |
| (2, 1) | $\psi(2S_1)$ | 3686 | $\Upsilon(2S_1)$ | 10023 |

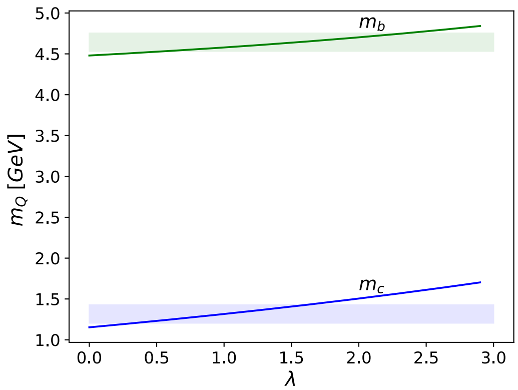


FIG. 2. Charm (lower blue line) and bottom (upper green line) quark masses in MeV as functions of $\lambda$ extracted from Eq. (27) for $\sigma = 0.2\ \mathrm{GeV}^2$. Shaded areas correspond to Eq. (8).

The results are shown in Fig. 1. We have checked our numerical results by comparing them with two semianalytical solutions: one when we solve the Airy equation and treat the Coulomb part as a perturbation, and another when we solve the Coulomb part and treat the confining part as a perturbation.

Next, we fix $\sigma$ and find the $c$- and $b$-quark masses as functions of $\lambda$ from the average ground-state masses:

$$\bar{M}_{Q\bar{Q}} = 2m_Q + \left(\frac{\sigma^2}{m_Q}\right)^{1/3} \zeta_1(\lambda). \tag{27}$$

The result is plotted in Fig. 2 for $\sigma = 0.2\ \mathrm{GeV}^2$. We see a rather moderate dependence of the heavy-quark masses on $\lambda$. The shaded areas show the mass limits of Eq. (8) that follow from the heavy baryon phenomenology in the present approach [5]. We see that the heavy-quark masses extracted from charmonia or heavy baryons are compatible, which proves the consistency of our approach.

Then, from the hyperfine splitting we find the value of $\alpha_s(m_Q)$,

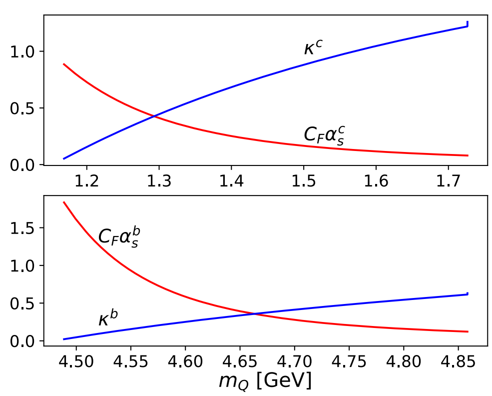


FIG. 3. Dependence of $C_F\alpha_s$ (red) and $\kappa$ (blue) on the heavy-quark mass for $\sigma = 0.2\ \mathrm{GeV}^2$, for the charm (upper panel) and bottom (lower panel). The point where the two lines cross corresponds to the model heavy-quark mass for a given string tension $\sigma$.

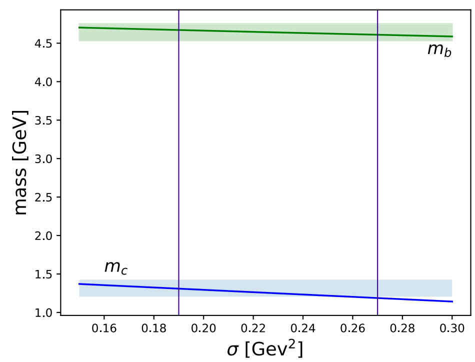


FIG. 4. Charm (lower blue line) and bottom (upper green line) quark masses in GeV as functions of $\sigma$ obtained from the fits to $1S$ states. Shaded areas correspond to Eq. (8). Vertical lines correspond to the best fits to $2S$ states: charm (left) and bottom (right); see Sec. III C.

$$\delta_{\mathrm{hf}} E_1(Q\bar{Q}) = \frac{2}{3} C_F \alpha_s(m_Q) \frac{\sigma}{m_Q} c_1^2(\lambda), \tag{28}$$

as a function of $\lambda$.

Since for a given $\lambda$ the quark mass $m_Q$ is fixed by Eq. (27), we can compute $\kappa_Q(\lambda)$ for both the charm and bottom from Eq. (18). However, $\kappa_Q(\lambda) = C_F\alpha_s(m_Q, \lambda)$, and therefore we can find $\lambda_Q^{\mathrm{sol}}$ for which this equality is satisfied. Since there is a one-to-one correspondence between $\lambda_Q$ and $m_Q$ (see Fig. 2), in Fig. 3 we plot $\kappa$ and $C_F\alpha_s$ in terms of the corresponding charm (top panel) and bottom (bottom panel) mass for $\sigma = 0.2\ \mathrm{GeV}^2$. Two lines cross at the quark mass corresponding to $\lambda_Q^{\mathrm{sol}}$.

In this way, for a given $\sigma$ we find unique values of $m_{c,b}(\sigma)$ and $\alpha_s(m_{c,b}(\sigma))$ that fit $1S$ ground-state quarkonia masses. The results are plotted in Figs. 4 and 5. We see that the quark mass dependence on $\sigma$ is relatively weak, and that masses extracted from $Q\bar{Q}$ mesons fall within the range (8) corresponding to the baryonic fits. This proves the consistency of our approach which combines the soliton model with the

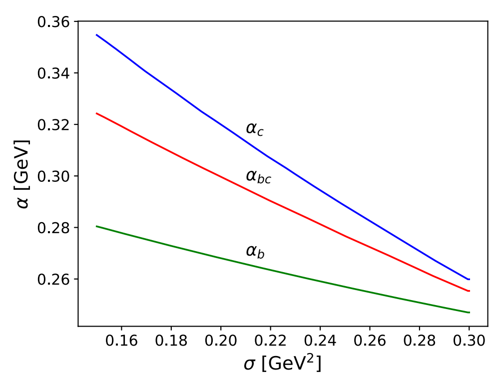


FIG. 5. Strong coupling constants $\alpha_s(2\mu)$ for charm (upper blue line) and bottom (lower green line), and for $\mu$ equal to the reduced mass of the $bc$ system (middle red line; see Sec. III C) as functions of the string tension $\sigma$.

nonrelativistic theory of heavy-quark bound states. Nevertheless, the $m_b - m_c$ mass difference changes in this $\sigma$ range by about 100 MeV, which (as we will see) is a source of uncertainty in the determination of the $cb$ tetraquark mass.

### C. Numerical results for quarkonia

Since all parameters are now fixed from the ground states, excited-state masses are predictions. Our results are plotted in Fig. 6. We see that first excited states in the charm and bottom sectors cannot be fitted by the same value of $\sigma$. The best fit for charmonia requires $\sigma_c \simeq 0.19\ \mathrm{GeV}^2$, while in the bottom sector $\sigma_b \simeq 0.27\ \mathrm{GeV}^2$. This agrees quite well with the results of global fits of Ref. [17], which give $0.164 \pm 0.011\ \mathrm{GeV}^2$ and $0.207 \pm 0.011\ \mathrm{GeV}^2$, respectively. Still, the error on excited charmonia masses at $\sigma = \sigma_b$ or bottomonia masses at $\sigma = \sigma_c$ is of the order of 70 MeV, i.e., 2% in the case of charmonia and less than 1% for bottomonia. We therefore restrict the range of the string tension to

$$0.19\ \mathrm{GeV}^2 \leq \sigma \leq 0.27\ \mathrm{GeV}^2, \tag{29}$$

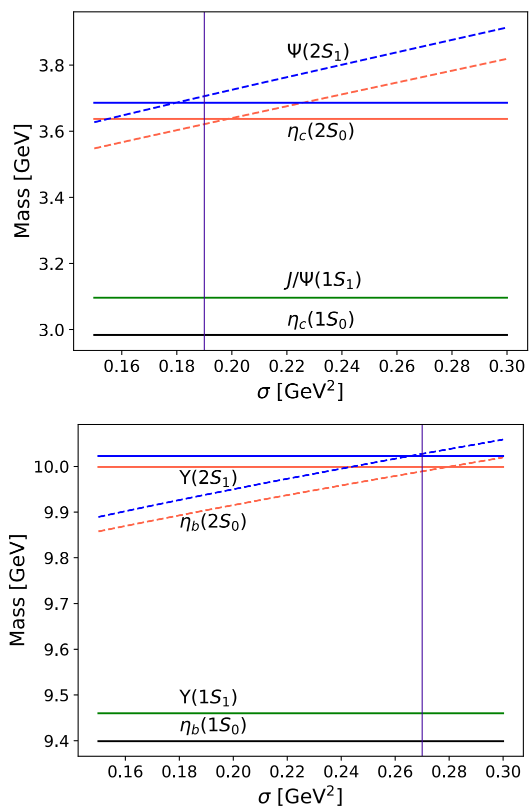


FIG. 6. Masses of the lowest $S$ state charmonia (upper panel) and bottomonia (lower panel) listed in Table II. Experimental data are shown by solid lines (from bottom to top): $\eta(1S_0)$ (black), $J/\Psi(1S_1)$ or $\Upsilon(1S_1)$ (green), $\eta(2S_0)$ (red) and $\Psi(2S_1)$ or $\Upsilon(2S_1)$ (blue). Dashed lines correspond to the fits described in the text (color encoding as in the case of experimental data). $1S$ states are used as input. Vertical lines indicate the values of $\sigma$ for which $2S$ mesons are best reproduced.

which in terms of the quark masses corresponds to

$$\begin{aligned} 1.19\ \mathrm{GeV} &\leq m_c \leq 1.31\ \mathrm{GeV}, \\ 4.61\ \mathrm{GeV} &\leq m_b \leq 4.67\ \mathrm{GeV}, \end{aligned} \tag{30}$$

which narrows the allowed range (8) following from the fits to heavy baryons.

We should stress once again that the above result is by no means trivial. Quark masses obtained from baryon spectra could in principle differ from dynamical inference from the meson sector. The fact that both sectors are compatible reinforces confidence in the consistency of the current approach.

We can now easily predict the masses of $c\bar{b}$ or $\bar{c}b$ mesons, two of which, namely, the spin-0 $B_c^+(1S_0, 6274.5)$ and $B_c^\pm(2S_0, 6871.2)$ mesons, are listed in the PDG [18]. To this end, we need to estimate the value of $\alpha_s(2\mu)$, where $\mu$ is the reduced mass (15) of the $cb$ system. To this end, we use the evolution formula

$$\alpha_s(m_b) = \frac{\alpha_s(m_c)}{1 + \frac{\beta_0}{2\pi}\alpha_s(m_c)\ln(m_b/m_c)}, \tag{31}$$

which allows us to compute the model $\beta_0$ as a function of the string tension,[3]

$$\beta_0 = 2\pi \frac{1/\alpha_s(m_b) - 1/\alpha_s(m_c)}{\ln(m_b/m_c)}. \tag{32}$$

From this we obtain $\alpha_s(2\mu)$, which is plotted as a red line in Fig. 5. The resulting masses are shown in Fig. 7. For the known spin $s = 0$ mesons, we have

$$\begin{aligned} 6.26\ \mathrm{GeV} &\leq m(B_c(1S_0, 6.275)) \leq 6.28\ \mathrm{GeV}, \\ 6.83\ \mathrm{GeV} &\leq m(B_c(2S_0, 6.871)) \leq 6.97\ \mathrm{GeV}, \end{aligned} \tag{33}$$

where the limits correspond to (29). We also predict for the spin $s = 1$ states

$$\begin{aligned} 6.32\ \mathrm{GeV} &\leq m(B_c(1S_1)) \leq 6.34\ \mathrm{GeV}, \\ 6.87\ \mathrm{GeV} &\leq m(B_c(2S_1)) \leq 7.02\ \mathrm{GeV}. \end{aligned} \tag{34}$$

The best fit, shown by the vertical line in Fig. 7, is for $\sigma = 0.21\ \mathrm{GeV}^2$, giving for spin $s = 1$ $M_{b\bar{c}}(1S_1) = 6.32$ GeV and $M_{b\bar{c}}(2S_1) = 6.91$ GeV. For the most recent survey of $B_c$ states, see Ref. [42].

In summary, we have fixed Cornell potential parameters from the $c\bar{c}$ charmonia and $b\bar{b}$ bottomonia spectra and computed without any further inputs the masses of the

[3]Remember that quark masses are in one-to-one correspondence with the string tension.

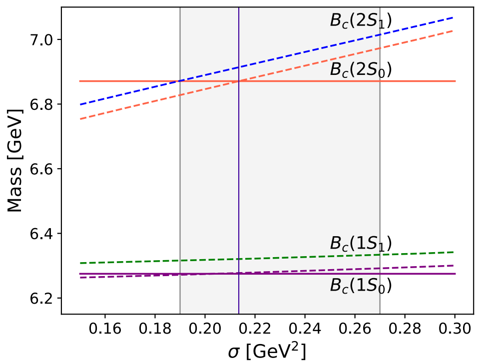


FIG. 7. Predicted masses of $B_c$ mesons as functions of the string tension $\sigma$ shown as dashed lines: (from noffom to top) $B_c(1S_0)$ (magenta), $B_c(1S_1)$ (green), $B_c(2S_0)$ (red) and $B_c(2S_1)$ (blue). Solid lines denote the two known spin $s = 0$ mesons $B_c^+(1S_0, 6274.5)$ and $B_c^{\pm}(2S_0, 6871.2)$ [18]. Vertical lines indicate the values of $\sigma$ for which both $B_c$ mesons are best reproduced. Shaded area corresponds to the limits of Eq. (29).

ground-state $c\bar{b}$ (or $\bar{c}b$) mesons that for the experimentally measured states agree very well with data.

### D. Numerical results for diquarks

Having constrained the parameters of the Cornell potential, we can now—with the help of Eqs. (24) and (23)—compute the diquark masses. In Fig. 8 we plot $cc$ and $bb$ spin $s = 1$ diquark masses as functions of $m_{c,b}$ rather than $\sigma$. The results are very similar to those obtained previously in Ref. [5], with one difference, namely, the slope of the diquark masses obtained here is smaller than 1 (with respect to $m_Q$), whereas in Ref. [5] the slope was slightly larger than 1. This means that the tetraquark masses, which are proportional to $m_{\bar{Q}\bar{Q}} - m_Q$, decrease with $m_Q$, while in Ref. [5] they were increasing as functions of the heavy-quark mass. Numerically, however, the results are very similar and show a slower increase than the total mass of their constituents.

In Fig. 9 we plot $cb$ diquark masses for both spin 0 and spin 1 as functions of $m_c + m_b$. We see that, similar to $m_{cc}$, the diquark mass is smaller than the relevant meson mass. In the case of $m_{bb}$, the diquark mass is larger than the mass of $\Upsilon$.

## IV. TETRAQUARK MASSES

### A. Antitriplet masses

To compute tetraquark masses in flavor $\bar{\mathbf{3}}$, we use Eq. (10) and the numerical results for the diquark masses from the previous section. Since identical quarks have to be in the spin-1 state, antitriplet tetraquarks are $J^P = 1^+$. The results are plotted in Fig. 10. We see that charm tetraquark masses are above the threshold, while in the case of the bottom there are rather deeply bound states for both nonstrange and strange tetraquarks. The lightest nonstrange charm tetraquark is approximately 70–95 MeV above the threshold, while the strange one is 155–180 MeV above the

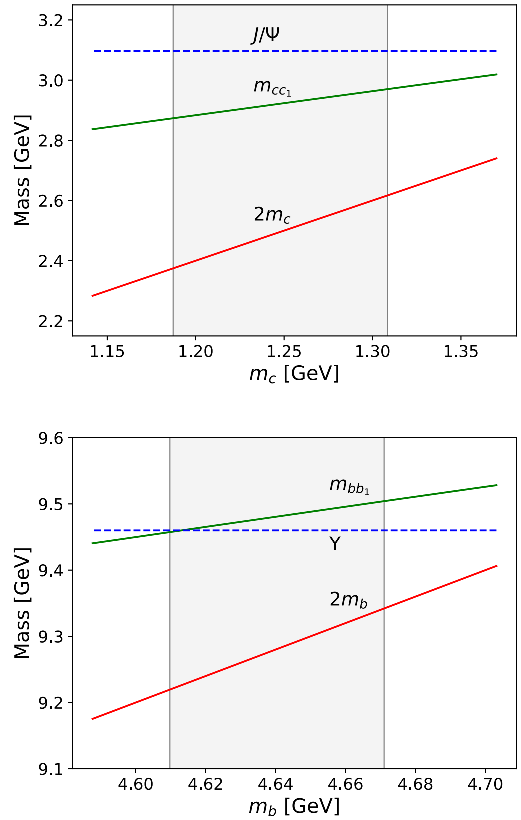


FIG. 8. Spin $s = 1$ charm (upper panel) and bottom (lower panel) diquark masses in GeV (green solid lines) as functions of $m_{c,b}$. Horizontal dashed lines show $J/\Psi$ and $\Upsilon$ masses, respectively, while red solid lines correspond to $2m_{c,b}$. Vertical lines indicate the values of $m_{c,b}$ corresponding to $\sigma$ for which $2S$ mesons are best reproduced. The shaded area corresponds to the limits of Eq. (30).

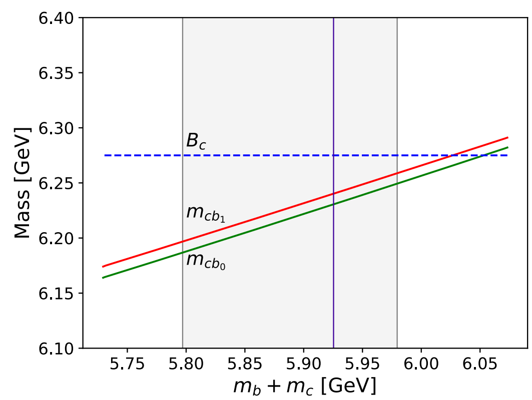


FIG. 9. Masses of $cb$ diquarks (solid lines) as functions of $m_c + m_b$. The lower line corresponds to $s = 0$ and the upper one to $s = 1$. The horizontal dashed line shows the $B_c(1S)$ mass. Vertical lines indicate the values of $m_b + m_c$ corresponding to $\sigma$ for which $B_c$ mesons are best reproduced. The shaded area corresponds to the limits of Eq. (30).

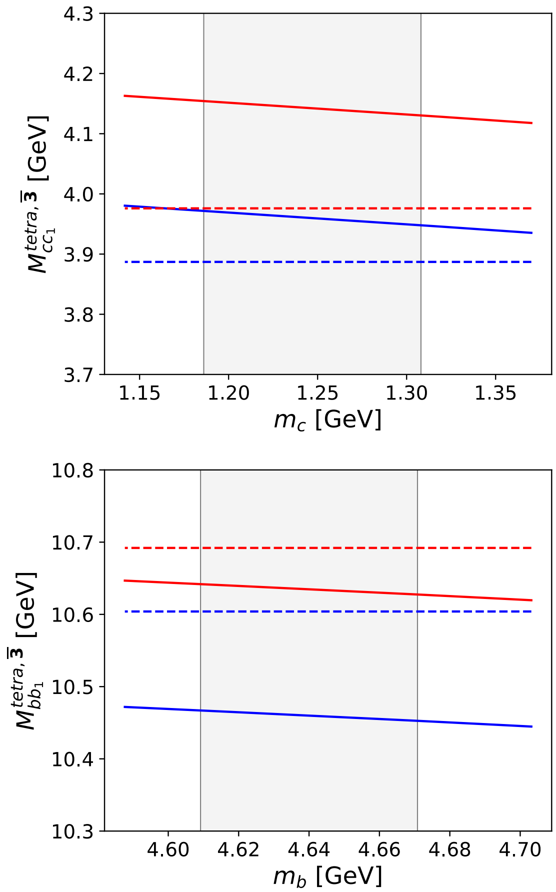


FIG. 10. Lightest nonstrange (solid blue, bottom) and strange (solid red, top) antitriplet tetraquark masses (charm: upper panel; bottom: lower panel) as functions of the heavy-quark mass. Horizontal dashed lines correspond to the pertinent thresholds (nonstrange: bottom; strange: top) given in Table I. Shaded areas correspond to the heavy-quark mass ranges (30). Vertical lines indicate the values of $m_{c,b}$ corresponding to $\sigma$ for which $2S$ mesons are best reproduced.

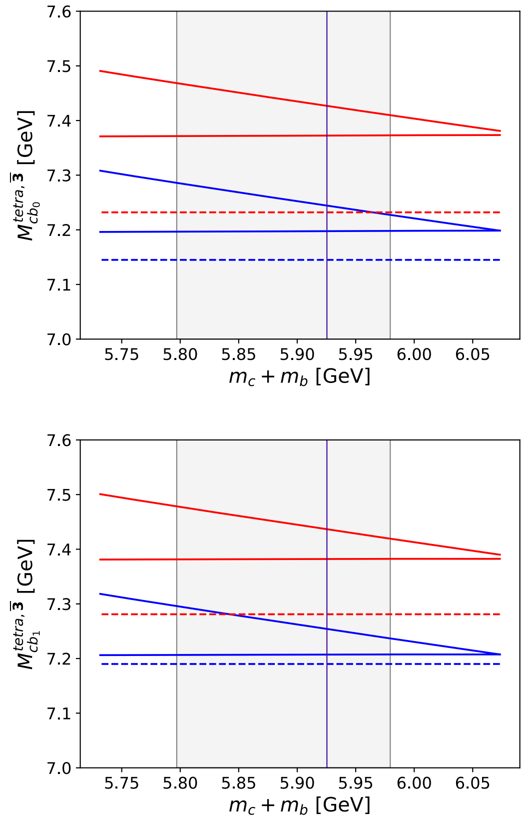


FIG. 11. Nonstrange (solid blue, bottom) and strange (solid red, top) antitriplet $cb$ tetraquark masses (spin 0: upper panel; spin 1: lower panel) as functions of $m_c + m_b$. Upper solid lines correspond to masses computed from the charm sector, while lower ones correspond to the $b$ sector. Horizontal dashed lines correspond to the pertinent thresholds (nonstrange: bottom; strange: top) given in Table I. Shaded areas show the heavy-quark mass ranges (30). Vertical lines indicate the values of $m_c + m_b$ corresponding to $\sigma$ for which $2S$ mesons are best reproduced.

threshold. On the contrary, bottom tetraquarks are bound by 140–150 MeV and 50–65 MeV for nonstrange and strange tetraquarks, respectively. These masses are in agreement with our previous work [5], except for the $m_{c,b}$ dependence, which (as explained in Sec. III D) has a different slope. Our results are also in a very good agreement with the predictions of Ref. [32].

Our new result in the present work is predictions for masses of $cb$ tetraquarks. The results are plotted in Fig. 11. Here, unlike in the case of identical quarks, both spin configurations of the $cb$ diquarks are possible: spin 0 is shown in the upper panel of Fig. 11 and spin 1 is shown in the lower panel. Moreover, we have two sets of predictions based on Eq. (10), where one can choose for $Q$ either $c$ or $b$. In principle, both determinations should coincide; however, we see a difference of the order of 100–30 MeV due to the variation of the $m_b - m_c$ mass difference with $\sigma$ discussed at the end of Sec. III B. The predictions from the bottom sector are lower and almost independent of the quark masses, while the predictions from the charm sector decrease with $m_c + m_b$.

The results of this section are summarized in Table III, where we quote our predictions for the tetraquark masses at quark masses corresponding to $\sigma$ for which $2S$ mesons are best reproduced. This means that for each sector we have in fact different $\sigma$. It is therefore surprising that the $m_c + m_b$ mass for $cb$ tetraquarks is practically equal to the sum of $m_c$ and $m_b$ masses determined from the $c$ and $b$ sectors separately (i.e., for different $\sigma$).

We see from Table III that only $bb$ tetraquarks, both strange and nonstrange, are bound, confirming results from Refs. [5,32]. Interestingly, the $cb$ nonstrange tetraquark of spin 1 is only 17–61 MeV above the threshold, which—given the accuracy of the model—does not exclude a weakly bound state. This is mainly due to the fact that the hyperfine splitting between spin-1 and spin-0$cb$ diquarks is only 10 MeV, while the difference of pertinent thresholds is 45 MeV. The fact that the $0^+$ $cb$ tetraquark could be bound was raised in Ref. [43].

TABLE III. Tetraquark masses in GeV at quark masses corresponding to $\sigma$ for which $2S$ mesons are best reproduced. The index $S$ refers to the diquark spin, which in the $\bar{\mathbf{3}}$ case is equal to the baryon spin. States below the threshold are displayed in boldface.

| Baryon | $QQ_S$ | Mass | Threshold | $m_Q$ or $m_c + m_b$ |
|---|---|---|---|---|
| $\Lambda_Q$ | $cc_1$ | 3.948 | 3.887 | 1.307 |
| $\Xi_Q$ | | 4.130 | 3.976 | |
| $\Lambda_Q$ | $bb_1$ | **10.467** | 10.604 | 4.609 |
| $\Xi_Q$ | | **10.642** | 10.692 | |
| $\Lambda_Q$ | $cb_0$ | 7.197–7.241 | 7.145 | 5.932 |
| | $cb_1$ | 7.207–7.251 | 7.190 | |
| $\Xi_Q$ | $cb_0$ | 7.327–7.424 | 7.232 | |
| | $cb_1$ | 7.382–7.334 | 7.281 | |

## B. Sextet masses

In the case of sextet tetraquarks, we have several spin states, since the soliton spin is $J = 1$ and the $QQ$ diquark spin is $S_{QQ} = 1$, and additionally 0 in the case of the $cb$ diquark. However, the pertinent spin splittings are very small. Indeed, for the $bc$ diquarks, spin splitting is of the order of 10 MeV (see Fig. 9) and the diquark-soliton spin splitting, depending on the diquark mass, is of the order of 60, 20, and 15 MeV for $cc$, $bc$, and $bb$ tetraquarks, respectively.

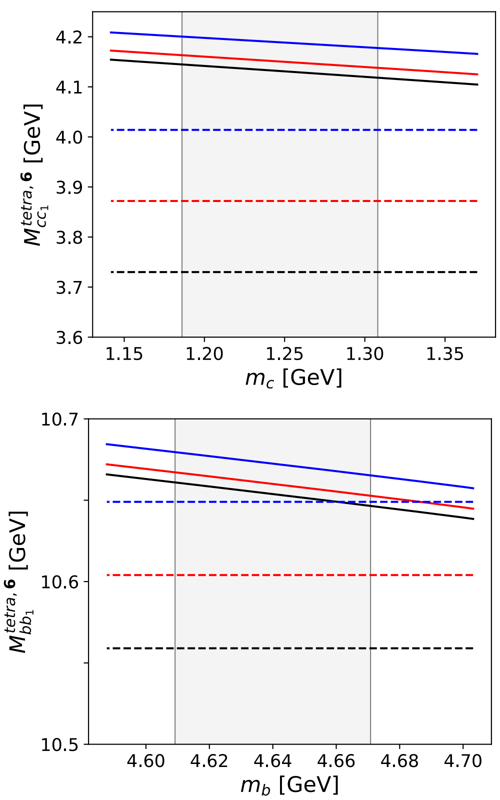


FIG. 12. Masses of $T_{cc}$ (upper panel) and $T_{bb}$ (lower panel) nonstrange sextet tetraquarks of spin 0, 1, and 2 (from bottom upwards) as functions of $m_Q$. Dashed lines show pertinent thresholds. Vertical lines indicate the values of $m_Q$ corresponding to $\sigma$ for which $2S$ mesons are best reproduced. The shaded area corresponds to the limits of Eq. (30).

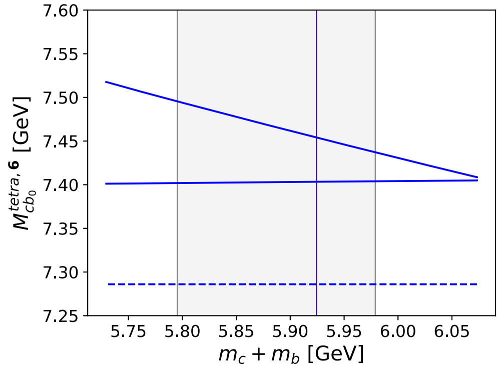


FIG. 13. Mass of the $T_{cb}$ nonstrange sextet tetraquark of spin 0 as a function of $m_c + m_b$. The upper line corresponds to the mass computed from the charm baryon spectrum, whereas the lower line corresponds to the bottom baryon (12). The dashed line shows the pertinent threshold. Vertical lines indicate the values of $m_c + m_b$ corresponding to $\sigma$ for which the $2S$ $B_c$ meson is best reproduced. The shaded area corresponds to the limits of Eq. (30).

Therefore, in the following we show only some representative plots for nonstrange sextet tetraquarks. For tetraquarks with nonzero strangeness, these curves have to be shifted upwards by the mass difference between heavy baryons used as a reference [see Eq. (12)] and the pertinent thresholds have to be replaced by the ones from Table I.

In Fig. 12 we plot nonstrange $cc$ and $bb$ tetraquark masses. In this case, tetraquarks have spin 0, 1, or 2, and they are shown by blue, orange, and green (from bottom to top), respectively. Pertinent thresholds are marked by dashed lines. In both cases, no bound states exist. These results are in agreement with our previous estimates from Ref. [5].

In Fig. 13 we plot the nonstrange $cb$ tetraquark mass for a diquark of spin 0, and therefore the tetraquark spin is $s = 1$. We see again that two different mass estimates based on $c$ or $b$ baryons in Eq. (12) differ by 15–95 MeV. In order to illustrate the pattern of spin splittings, in Table IV we show predictions for all spin combinations at the aggregate mass $m_c + m_b = 5.932$ GeV. We see that the spin splittings at this mass are of the order of 10 MeV, whereas the uncertainty due to the reference baryon (charm or bottom) is of the order of 50 MeV. All states are above the threshold.

TABLE IV. Masses (in GeV) of nonstrange sextet $cb$ tetraquarks of spin $s$ for $\bar{c}\,\bar{b}$ diquark of spin $S_{\bar{c}\bar{b}}$.

| $S_{\bar{c}\bar{b}}$ | 0 | 1 |
|---|---|---|
| $s = 0$ | ⋯ | 7.39–7.44 |
| $s = 1$ | 7.40–7.45 | 7.40–7.45 |
| $s = 2$ | ⋯ | 7.42–7.47 |

## V. SUMMARY AND CONCLUSIONS

In this work, we have calculated the masses of heavy tetraquarks in a model in which the light sector is described by a chiral quark-soliton model, while the mass of the heavy diquark is calculated from the Schrödinger equation with the Cornell potential including spin interactions. In this way, we extended our previous analysis [5] where the explicit spin interaction was ignored and only tetraquarks with identical heavy antiquarks were considered. Since we have been interested in $1S$ ground states only, there was no need to include tensor and spin-orbit couplings. We have developed our own fitting procedure to fix the parameters of the Cornell potential, including heavy-quark masses, from the charmonium and bottomonium spectra. The resulting quark masses are in agreement with the quark masses extracted from the heavy baryon spectra calculated in the framework of the $\chi$QSM; see Fig. 4. This proves the consistency of our approach. Moreover, our parameters are in a reasonable agreement with the results from the global fits [17].

Furthermore, having all parameters fixed, we calculated $B_c$-meson masses with no additional input. These predictions agree very well with two experimentally known cases; see Eq. (33). This reassured us that the parameters of the Cornell potential were correctly extracted from the $\bar{c}c$ and $\bar{b}b$ spectra, and that the interpolation to the $\bar{c}b$ system was correctly performed. We also predicted masses of the $B_c$ vector mesons (34).

In order to compute diquark masses, we appropriately rescaled the color factors entering the Cornell potential, since the two antiquark color charges couple in this case to an SU(3) triplet rather than to a singlet. The results are given in Sec. III D.

Heavy tetraquarks can be characterized according to the SU(3) classification of heavy baryons, in which the heavy quark $Q$ has been replaced by an antidiquark. Therefore, the mass formulas (10) and (12) include heavy baryon masses and diquark masses and the spin-spin interaction. They are analogous to the phenomenological mass formulas of Ref. [32].

Our main conclusion is that only the $bb$ tetraquarks are bound, both nonstrange and strange. Unfortunately, the $cb$ system is not heavy enough to create a bound state. One of the main motivations of the present paper was to check whether $cb$ tetraquarks exist. There is still a possibility that a strange $cb$ tetraquark might exist, since—given the accuracy of the present approach—our predictions lie very close to the $\bar{D}^{*0}\bar{B}_s^0$ threshold.

In view of these findings, it seems likely that the LHCb charm tetraquark is a kind of molecular configuration [44,45], which is beyond our present approach.

## ACKNOWLEDGMENTS

This research has been Supported by the Polish National Science Centre Grant No. 2017/27/B/ST2/01314.

[1] R. Aaij *et al.* (LHCb Collaboration), Observation of an exotic narrow doubly charmed tetraquark, Nat. Phys. **18**, 751 (2022).
[2] R. Aaij *et al.* (LHCb Collaboration), Study of the doubly charmed tetraquark $T_{cc}^+$, Nat. Commun. **13**, 3351 (2022).
[3] M. Karliner, J. L. Rosner, and T. Skwarnicki, Multiquark states, Annu. Rev. Nucl. Part. Sci. **68**, 17 (2018).
[4] H.-X. Chen, W. Chen, X. Liu, Y.-R. Liu, and S.-L. Zhu, An updated review of the new hadron states, Rep. Prog. Phys. **86**, 026201 (2023).
[5] M. Praszalowicz, Doubly heavy tetraquarks in the chiral quark soliton model, Phys. Rev. D **106**, 114005 (2022).
[6] D. Diakonov, V. Y. Petrov, and P. V. Pobylitsa, A chiral theory of nucleons, Nucl. Phys. **B306**, 809 (1988).
[7] C. V. Christov, A. Blotz, H. C. Kim, P. Pobylitsa, T. Watabe, T. Meissner, E. Ruiz Arriola, and K. Goeke, Baryons as nontopological chiral solitons, Prog. Part. Nucl. Phys. **37**, 91 (1996).
[8] R. Alkofer, H. Reinhardt, and H. Weigel, Baryons as chiral solitons in the Nambu-Jona-Lasinio model, Phys. Rep. **265**, 139 (1996).
[9] V. Petrov, Soliton model for baryons, Acta Phys. Pol. B **47**, 59 (2016).
[10] G. S. Yang, H. C. Kim, M. V. Polyakov, and M. Praszałowicz, Pion mean fields and heavy baryons, Phys. Rev. D **94**, 071502 (2016).
[11] H. C. Kim, M. V. Polyakov, and M. Praszałowicz, Possibility of the existence of charmed exotica, Phys. Rev. D **96**, 014009 (2017).
[12] H. C. Kim, M. V. Polyakov, M. Praszalowicz, and G. S. Yang, Strong decays of exotic and nonexotic heavy baryons in the chiral quark-soliton model, Phys. Rev. D **96**, 094021 (2017); **97**, 039901(E) (2018).
[13] M. V. Polyakov and M. Praszalowicz, Landscape of heavy baryons from the perspective of the chiral quark-soliton model, Phys. Rev. D **105**, 094004 (2022).
[14] M. Praszałowicz and M. Kucab, Invisible charm exotica, Phys. Rev. D **107**, 034011 (2023).
[15] M. Praszalowicz, Doubly heavy $QQ$ tetraquarks, Acta Phys. Pol. B Proc. Suppl. **13**, 103 (2020).
[16] E. Eichten, K. Gottfried, T. Kinoshita, K. D. Lane, and T. M. Yan, Charmonium: The model, Phys. Rev. D **17**, 3090 (1978); **21**, 313(E) (1980).

[17] V. Mateu, P. G. Ortega, D. R. Entem, and F. Fernández, Calibrating the Naïve Cornell model with NRQCD, Eur. Phys. J. C **79**, 323 (2019).
[18] R. L. Workman *et al.* (Particle Data Group), Review of particle physics, Prog. Theor. Exp. Phys. **2022**, 083C01 (2022).
[19] B. A. Gelman and S. Nussinov, Does a narrow tetraquark $cc\bar{u}\bar{d}$ state exist?, Phys. Lett. B **551**, 296 (2003).
[20] J. Carlson, L. Heller, and J. A. Tjon, Stability of dimesons, Phys. Rev. D **37**, 744 (1988).
[21] A. V. Manohar and M. B. Wise, Exotic QQqq states in QCD, Nucl. Phys. **B399**, 17 (1993).
[22] N. Isgur and M. B. Wise, Spectroscopy with heavy quark symmetry, Phys. Rev. Lett. **66**, 1130 (1991).
[23] F. S. Navarra, M. Nielsen, and S. H. Lee, QCD sum rules study of $QQ - \bar{u}\,\bar{d}$ mesons, Phys. Lett. B **649**, 166 (2007).
[24] T. D. Cohen and P. M. Hohler, Doubly heavy hadrons and the domain of validity of doubly heavy diquark-anti-quark symmetry, Phys. Rev. D **74**, 094003 (2006).
[25] A. Esposito, M. Papinutto, A. Pilloni, A. D. Polosa, and N. Tantalo, Doubly charmed tetraquarks in $B_c$ and $\Xi_{bc}$ decays, Phys. Rev. D **88**, 054029 (2013).
[26] Y. Cai and T. Cohen, Narrow exotic hadrons in the heavy quark limit of QCD, Eur. Phys. J. A **55**, 206 (2019).
[27] M. Karliner and J. L. Rosner, Discovery of doubly-charmed $\Xi_{cc}$ baryon implies a stable $(bb\bar{u}\,\bar{d})$ tetraquark, Phys. Rev. Lett. **119**, 202001 (2017).
[28] S. S. Agaev, K. Azizi, B. Barsbay, and H. Sundu, The doubly charmed pseudoscalar tetraquarks $T^{++}_{cc;\bar{s}\,\bar{s}}$ and $T^{++}_{cc;\bar{d}\,\bar{s}}$, Nucl. Phys. **B939**, 130 (2019).
[29] S. S. Agaev, K. Azizi, B. Barsbay, and H. Sundu, Weak decays of the axial-vector tetraquark $T^{-}_{bb;\bar{u}\bar{d}}$, Phys. Rev. D **99**, 033002 (2019).
[30] H. J. Lipkin, A model independent approach to multi-quark bound states, Phys. Lett. B **172**, 241 (1986).
[31] J. P. Ader, J. M. Richard, and P. Taxil, Do narrow heavy multi-quark states exist?, Phys. Rev. D **25**, 2370 (1982).
[32] E. J. Eichten and C. Quigg, Heavy-quark symmetry implies stable heavy tetraquark mesons $Q_iQ_j\bar{q}_k\bar{q}_l$, Phys. Rev. Lett. **119**, 202002 (2017).
[33] E. Witten, Baryons in the $1/N$ expansion, Nucl. Phys. **B160**, 57 (1979).
[34] E. Witten, Current algebra, baryons, and quark confinement, Nucl. Phys. **B223**, 422 (1983); **B223**, 433 (1983).
[35] E. Guadagnini, Baryons as solitons and mass formulae, Nucl. Phys. **B236**, 35 (1984).
[36] P. O. Mazur, M. A. Nowak, and M. Praszalowicz, SU(3) extension of the Skyrme model, Phys. Lett. **147B**, 137 (1984).
[37] S. Jain and S. R. Wadia, Large $N$ baryons: Collective coordinates of the topological soliton in SU(3) chiral model, Nucl. Phys. **B258**, 713 (1985).
[38] A. Blotz, D. Diakonov, K. Goeke, N. W. Park, V. Petrov, and P. V. Pobylitsa, The SU(3) Nambu-Jona-Lasinio soliton in the collective quantization formulation, Nucl. Phys. **A555**, 765 (1993).
[39] M. Karliner and J. L. Rosner, Baryons with two heavy quarks: Masses, production, decays, and detection, Phys. Rev. D **90**, 094007 (2014).
[40] M. Karliner and J. L. Rosner, Doubly charmed strange tetraquark, Phys. Rev. D **105**, 034020 (2022).
[41] A. Nakamura and T. Saito, QCD color interactions between two quarks, Phys. Lett. B **621**, 171 (2005).
[42] X. J. Li, Y. S. Li, F. L. Wang, and X. Liu, Spectroscopic survey of higher-lying states of $B_c$ meson family, Eur. Phys. J. C **83**, 1080 (2023).
[43] X. Z. Weng, W. Z. Deng, and S. L. Zhu, Doubly heavy tetraquarks in an extended chromomagnetic model, Chin. Phys. C **46**, 013102 (2022).
[44] D. Janc and M. Rosina, The $T_{cc} = DD^*$ molecular state, Few-Body Syst. **35**, 175 (2004).
[45] N. Li, Z. F. Sun, X. Liu, and S. L. Zhu, Coupled-channel analysis of the possible $D^{(*)}D^{(*)}, \bar{B}^{(*)}\bar{B}^{(*)}$ and $D^{(*)}\bar{B}^{(*)}$ molecular states, Phys. Rev. D **88**, 114008 (2013).